



Stresses in repair welding of high-strength steels—part 2: heat control and stress optimization

Dirk Schröpfer¹ · Julien Witte¹ · Arne Kromm¹ · Thomas Kannengiesser^{1,2}

Received: 13 November 2023 / Accepted: 14 February 2024
© The Author(s) 2024

Abstract

In welding of high-strength steels, e.g. for foundations and erection structures of wind energy plants, unacceptable defects can occasionally be found in the weld area, which should be removed by thermal gouging and subsequent re-welding. High shrinkage restraint of repair welds may lead to crack formation and component failure, predominantly in interaction with degraded microstructures and mechanical properties due to repair cycles. This study aims for elaboration of recommendations for repair concepts appropriate to the stresses and materials involved to avoid cold cracking, damage and expensive reworking. In part 1 [1] of this study, systematic investigations of influences of shrinkage restraint on residual stresses and cold cracking risk during repair welding of two high-strength steels S500MLO for offshore application and S960QL for mobile crane structures were focussed. In this part 2, the microstructure, particularly hardness, and residual stresses due to gouging and influences of heat control parameters in repair welding are analysed. A clear reduction in residual stress after gouging can be observed, especially for the specimens with restrained transverse shrinkage. Gouging to a depth of approx. 2/3 of the seam height does not lead to a complete relaxation of the observed reaction forces. Particularly for the higher strength steel S960QL, there are pronounced areas influenced by the gouging process in which a degradation of the microstructure and properties should be assumed. Overall, the repair welds show a significant increase in the width of the weld and HAZ compared to the original weld, especially in the case of S960QL/G89. The repair welds show higher welding-induced stresses than the original welds, especially in the areas of the HAZ and the base metal close to the weld seam. This behaviour can be attributed overall to increased restraint conditions due to the remaining root weld or shorter gouge grooves. In good agreement with earlier investigations, the residual stresses transverse to the weld can be significantly reduced by upwardly limited working or interpass temperatures, and the reaction stresses resulting from high restraint conditions can be effectively counteracted. The influence of the heat input on the stress formation is low compared to the interpass temperature for both test materials.

Keywords Repair-welding · High-strength steels · Cold cracking · Residual stresses

1 Introduction

Modern high-strength fine-grained structural steels have to be applied increasingly in future wind energy applications to take into account growing plant sizes or installed power of wind turbines, which must be adapted for this capability

and also be manufacturable in a resource-efficient way [1, 2]. Welding production of these high-strength steels is challenging due to high-fidelity working ranges in terms of heat control. In particular, the high demands on the integrity of the welded joint with regard to the welding-related stresses and the degradation of the special microstructures of these steel grades must be taken into account in the welding process and through adequate heat control concepts [3–5]. This applies in particular to repair welds in the case that safety-relevant weld defects are detected during non-destructive testing of the components [4]. As described in part 1 of this study [1], the repair of welded components usually leads to very high stiffness conditions and thus to the excessive development of high tensile residual stresses in the weld area. In connection with degraded high-strength microstructures with low strain

Recommended for publication by Commission II - Arc Welding and Filler Metals

✉ Dirk Schröpfer
dirk.schroepfer@bam.de

¹ Bundesanstalt Für Materialforschung (BAM), Berlin, Germany

² Otto-Von-Guericke University, Magdeburg, Germany

reserves, these can lead to cold cracks, overload fractures and overall, to a poor performance of the welded component or premature failure. In many cases, no constructive measures, e.g. disassembly work prior to repair welding, can be considered to reduce the stiffness conditions, i.e. the restraint intensity of the welds [1, 4]. Therefore, it is crucial that the stiffness conditions, the resulting degraded microstructure and the resulting residual stresses are all carefully considered and investigated for high-strength steels when developing welding repair concepts or repair cycles, as shown in Fig. 1 [5]. In practice, decisions on the feasibility of a safe repair weld as well as on the procedure are mostly based on empirical values and the expertise of the manufacturing companies. Standards and regulations on weld qualification hardly give any concrete indications on an adequate repair strategy, and there is currently no consistent scientific data base to support this. The result of repeated thermal loading, thus, may be a detrimental impact on the special microstructure of the high-strength steel grades and an over-proportional degradation of the demanded properties.

During repair welding of the joint grooves, high local shrinkage restraint and global rigidity conditions are oftentimes the case due to the surrounding structure, leading to elevated residual stresses [6, 7]. These stresses during repair welding are particularly critical in high-strength fine-grained structural steels with regard to renewed cracking due to the specific properties and microstructure as well as the low strain reserves. There are standards and guidelines, e.g. EN 1011-2 [8], for crack-resistant and stress appropriate welding of fine-grain structural steels, whose recommendations and specifications for adequate heat control during welding (heat input, preheat and interpass temperatures) are based only on carbon equivalent concepts. In addition, these guidelines are based primarily on studies of free-shrinking laboratory specimens and lower/mild strength steels. Extensive investigations have already been carried out, especially to address high-strength steel microstructures and considering realistic restraint and heat dissipation conditions comparable to actual component welds [9–11]. Significant influences of heat input, welding

process and restraint conditions on microstructure and welding-induced stresses have been quantified [12, 13]. Experimental and simulative studies have shown that post-weld heating instead of welding at elevated preheat temperature under high shrinkage restraint can have a significantly more favourable effect on the resulting residual stress level [14, 15]. The special features of weld repair as a result of the process-specific and design conditions require separate investigations for this purpose. Thermal gouging, for example, causes very high heating and cooling rates and, especially in multilayer welds, significant ductility and toughness losses in the areas of the heat-affected zone (HAZ) that are repeatedly heated to temperatures between Ac1 and Ac3 [16]. At the surface near areas of gouged grooves, the resulting short cooling times usually cause martensite formation and unacceptable hardening of the microstructure. Furthermore, the use of graphite electrodes at the joint edges leads to carbon enrichment, which according to [17] amounts up to 2% in the cutting edges. As a result, a significant change in the microstructure morphology of the weld and HAZ can be expected for the C-enriched areas during melting due to the subsequent repair welding combined with a strengthening of the weld metal. Therefore, the mechanical reworking of the joint flanks must also be checked in practice. Another focus should be placed on a possible overlap of the HAZ of the repair weld with the critical HAZ areas in multilayer welds and with the undercuts of the initial weld. Further studies have already shown that the stress level increases with each repair cycle, especially in the HAZ [4, 18], which makes it even more important that as few repair cycles as possible are necessary to eliminate weld defects.

Consequently, based on the results of the first part [1], this second part of the study deals with the resulting microstructures, in particular the hardness, due to gouging and repair welding. Also, the development of residual stresses as a function of the length of the gouging groove or the prevailing restraint conditions as well as the influence of the welding heat control is evaluated. The investigations were performed with both relevant steel grades S500MLO for offshore applications and S960QL typically used for mobile, crawler or ship

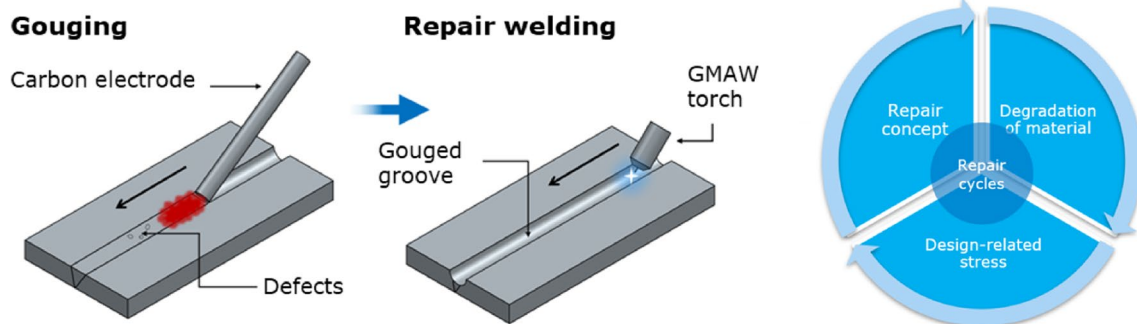


Fig. 1 Scheme of repair process and impact on structural integrity losses per repair cycle

cranes. The aim is to obtain information on how heat control can be optimised in terms of appropriate repair concepts.

2 Approach and experimental data

2.1 Restraint analysis of specimen dimensions for repair welding

Based on the results of the component analyses of part 1, the restraint intensities (according to the restraint intensity concept by Satoh et al. [19]) of gouged specimens were analysed numerically using structural mechanic calculations.

In order to represent relevant repair cases sufficiently close to the application, short areas with weld defects were assumed for the material S500MLO. S500MLO is more resistant to cold cracking than S960QL as weld tests under restraint showed in [1]. Thus, a greater test severity for the repair welding tests was chosen. The gouged length L_A is about 3/4 of the weld length of the original weld L_S for the self-restrained specimens P2 and P3, cf. Figure 2a, leading to restraint intensities of approx. $R_{Fy} = 15 \text{ kN}/(\text{mm mm})$ and $R_{Fy} = 30 \text{ kN}/(\text{mm mm})$, respectively. It should be noted that the restraint intensity is assumed to be somewhat higher, since only 2/3 of the weld height were gouged, approx. to the depth of the root layer, which additionally restrains the shrinkage to a certain extend.

In the case of S960QL, which is much more sensitive to cold cracking [1], longer areas were assumed to be gouged. The gouged length is equal to the weld length of the original weld, cf. Figure 2b. Thus, this higher-strength material is also taken into account by a lower test severity as well as a possible more frequent occurrence of weld defects at the beginning and

end of the weld. Thus, the self-restrained slot specimens P2 and P3 have a restraint intensity of $R_{Fy} = 10 \text{ kN}/(\text{mm mm})$ and $R_{Fy} = 20 \text{ kN}/(\text{mm mm})$, respectively, which is also assumed to be somewhat higher due to gouging of the weld height of 2/3 of the original weld. Figure 2c shows the specimens according to [1] with indicated gouging lengths.

2.2 Materials

In the experiments, welded free shrinking and self-restrained slot specimens made of S500MLO (EN 10225–1) and S960QL (EN 10025–6) were gouged and welded with solid wires G 50 7 M21 4Mo (ISO 12341) and G 89 6 M Mn4Ni2CrMo (ISO 16834-A), respectively. Table 1 presents the chemical compositions and mechanical properties of the applied steel grades base materials (BM) and weld metals (WM), according to [1].

2.3 Gouging experiments

The welded specimens (free shrinking/P1 and slotted specimens/P2 and 3) were each gouged using carbon arc gouging. The gouging tests were carried out manually, down to the depth of the root layer (i.e. over approx. 50–70% of the weld seam height). The weld metal was mainly driven out completely to the weld seam flank on one side. On the opposite side, the influence of the gouging and the subsequent repair welding on the remaining weld metal could be investigated by the incomplete gouging. The specimens of grade S960QL/G89 were gouged over the entire weld length, and for steel grade S500MLO/G50, to about 3/4 of the original weld length, as stated above. Table 2 gives an overview of the corresponding power sources, electrode types and gouging parameters, which differ slightly for the two different

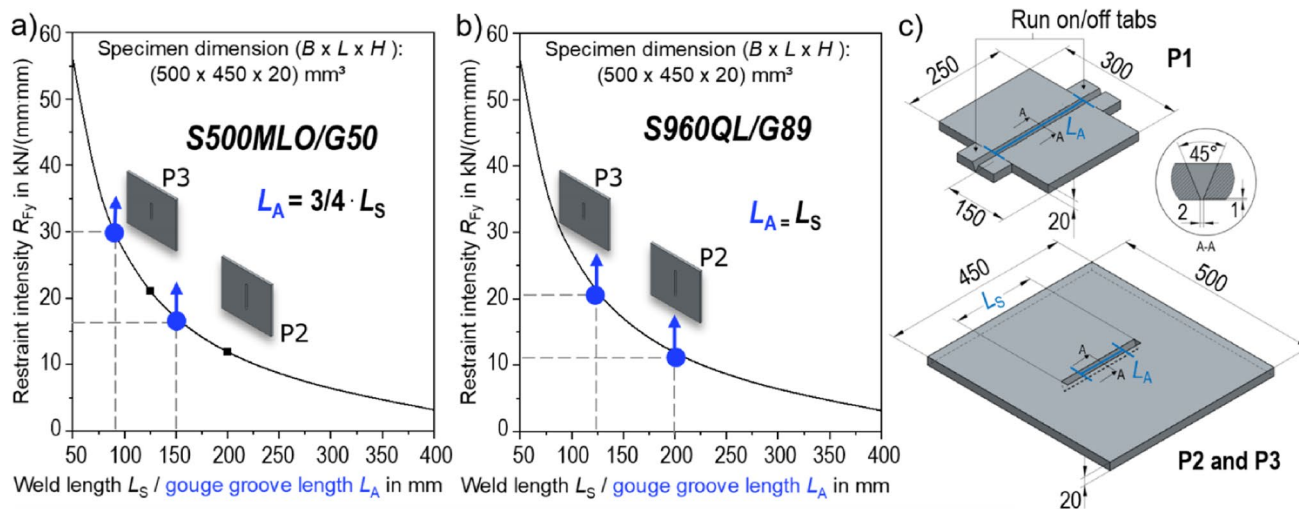


Fig. 2 Restraint intensity R_{Fy} vs. weld and gouge groove lengths L_S and L_A for **a** S500MLO/G50 and **b** S960QL/G89 for **c** different specimen types P1–3

Table 1 Chemical composition of BM, deposited WM (measured via optical emission spectrometer, Fe balanced) and mechanical properties (0.2% yield strength, $R_{p0.2}$, ultimate tensile strength R_m , elongation at fracture A_5 at room temperature; Charpy notched impact strength A_5 at given temperature)

Base material/ welding wire	C	Si	Mn	P	S	Cr	Cu	Mo	Ni	V	Nb	Ti	$R_{p0.2}$ in MPa	R_m in MPa	A_5 in %	A_5 in J
S500MLO/ 20 mm	0.05	0.34	1.81	0.009	<0.002	0.17	0.02	0.13	0.11	0.006	0.040	0.008	546	736	22	324 @ -40 °C
G 50	0.10	0.69	1.82	0.003	0.011	0.03	0.04	0.43	0.02	0.001	0.002	0.002	607	637	18	60 @ -70 °C
S960QL/20 mm	0.16	0.21	1.18	0.009	<0.002	0.20	0.010	0.58	0.05	0.047	0.015	0.001	1006	1053	17	96 @ -40 °C
G 89	0.11	0.81	1.80	0.005	0.009	0.36	0.022	0.57	2.24	0.006	0.001	0.084	1040	1108	15	62 @ -60 °C

materials. With the selection of an electrode diameter of approx. 8 mm, comparable resulting heat input could be implemented for the materials. A measurement of current and voltage during gouging was carried out. The measured values were averaged over the number of gouging passes until the final geometry was reached. The steel grade S500MLO/G50, which is less critical in terms of microstructure, could be gouged without preheating at room temperature (RT). For the higher strength steel S960QL/G89, due to its special comparatively sensitive microstructure and properties, the specimens were completely preheated with an oxy-acetylene torch to about 100 °C. For the subsequent repair welds, the flanks of the gouging groove were reworked using compressed air hammers, chisels or, if necessary, grinders, cf. Figure 3c–e, as is the case in industrial application.

2.4 Repair welding experiments

In the repair welding experiments, the gouged specimens made of both steel grades were rewelded with the solid wires G 50 7 M21 4Mo (ISO 12341) and G 89 6 M Mn4Ni2CrMo (ISO 16834-A), respectively, using machined MAG welding, cf. Figure 4.

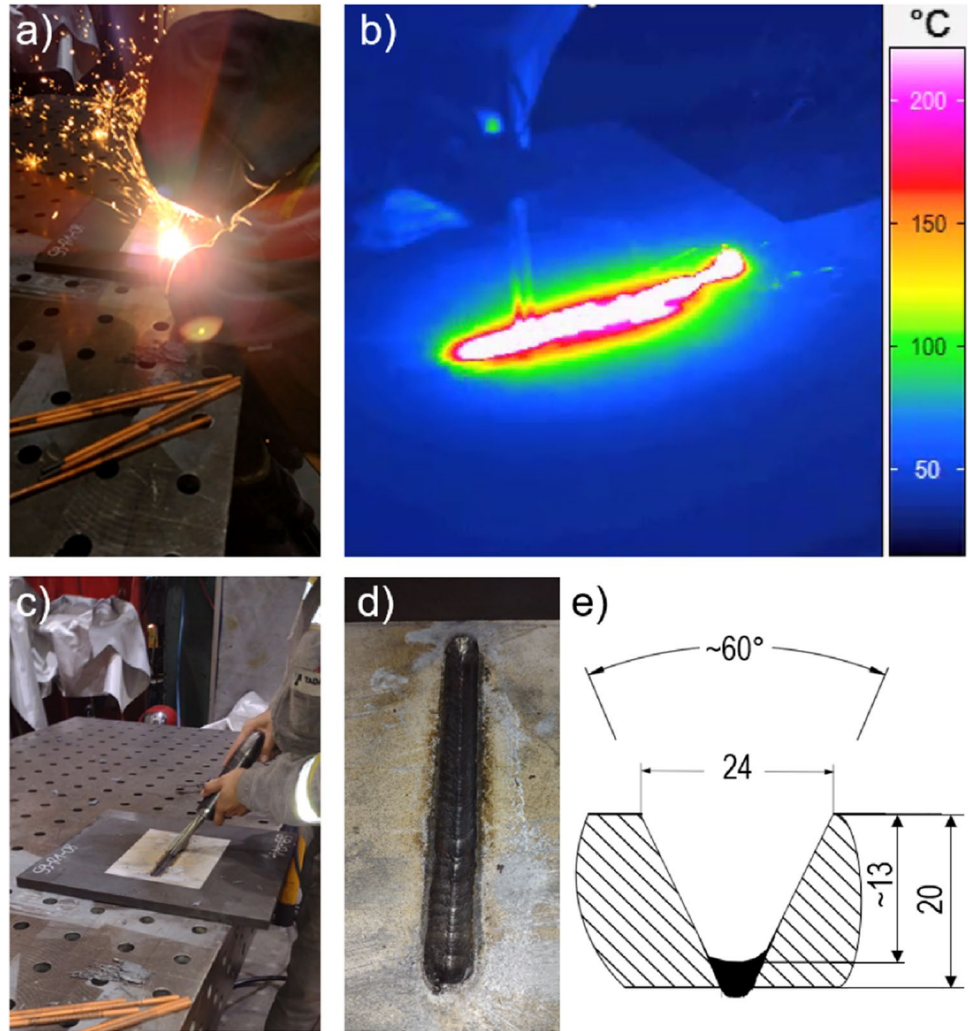
The test set-up and the instrumentation of the repair welding tests were carried out in the same way as described in [1] with equivalent welding parameters, see Fig. 4b. The preheating was carried out locally in the welding area by means of an oxy-acetylene flame. The preheating and inter-pass temperatures were monitored using type-K thermocouples. The $\Delta t_{8/5}$ cooling times were determined by means of a two-colour pyrometer and the actual values of welding current and voltage were determined via a Weld QAS system. The tests included a full factorial test matrix (DoE), cf. Figure 5. The influence of heat input and working temperature, as well as the restraint intensity or specimen shape P1-3, cf. Section 2.1, on the level and distribution, in particular of the residual stresses transverse to the weld seam after repair welding, can be statistically represented appropriately by this test method. In addition, the influence of heat control on the microstructure of the repair weld was determined by taking transverse sections of the specimens with minimum, medium and maximum cooling times, cf. Figure 5.

2.5 Residual stress analysis

The longitudinal and transverse residual stresses of the repair welds were analysed using X-ray diffraction (XRD, [20]) in accordance with the analysis in [1], cf. Figure 6. Focus was on transverse residual stresses at the major number of all specimens—as the restraint condition transverse to the weld direction was varied in systematic manner. XRD analysis was performed along a measuring track at the specimen centre

Table 2 Fixed parameter sets for gouging experiments for both steel grades

Steel grade	Power source (manufacturer, type)	Electrode (manufacturer, $\varnothing \times$ length in mm)	p in bar	l in A	U in V	T_p in °C
S500MLO/G50	Fronius TransSynergic 5000	Binzel – ABIARC, 8.0 \times 305	~5	~452	~40	RT
S960QL/G89	CLOOS QINEO WD PULSE	ESAB – ARCAIR, 7.9 \times 305	~5	~380	~60	100

Fig. 3 **a** Manual thermal gouging, **b** Temperature map during gouging, **c** Mechanical reworking of the gouged groove (**d**), **e** Approximated gouge groove dimensions

axis transverse to the welding direction (up to ± 100 mm from the weld centre). A semi-automatic measuring system was used, applying the $\sin^2\Psi$ -method (CrK α ; collimator, $D=2$ mm; Ψ -steps, 7; Ψ -range, $\pm 45^\circ$).

3 Results

3.1 Gouging results

Figure 7 shows the groove (a, e), the cross-sections (b, f) with detail of the gouging HAZ (c, g) and hardness distributions

(d, h) of gouged, non-mechanically post-treated, free-shrinking weld specimens of S500MLO/G50 and S960QL/G89. The maps of the micro-hardness measurements (HV0.5) were determined by means of the UCI method (ultrasonic contact impedance). The remaining weld metal at the root and at the right seam flank is visible. In addition, a heat-affected zone caused by the thermal gouging process can be seen on the seam flanks, cf. Figure 7c and g. The HAZ due to gouging of the weld of S500MLO/G50 is presented by an approx. 1 mm wide, partly considerably hardened (400 to 450 HV0.5) area, cf. Figure 7c and d. The metallographic examinations of the transverse section (etching with 2% Nital) show the respective HAZ due to

Fig. 4 a Test set-up of the repair welding experiments. **b** $\Delta t_{8/5}$ cooling time range according to the heat control variation within the DoE. **c** Welding and heat control parameters

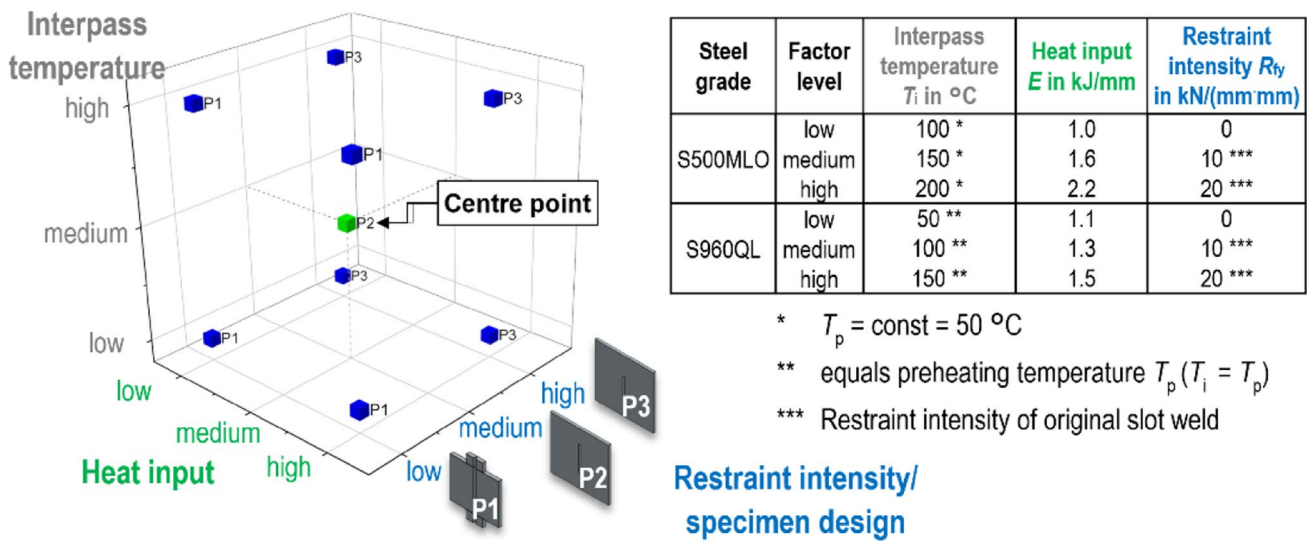
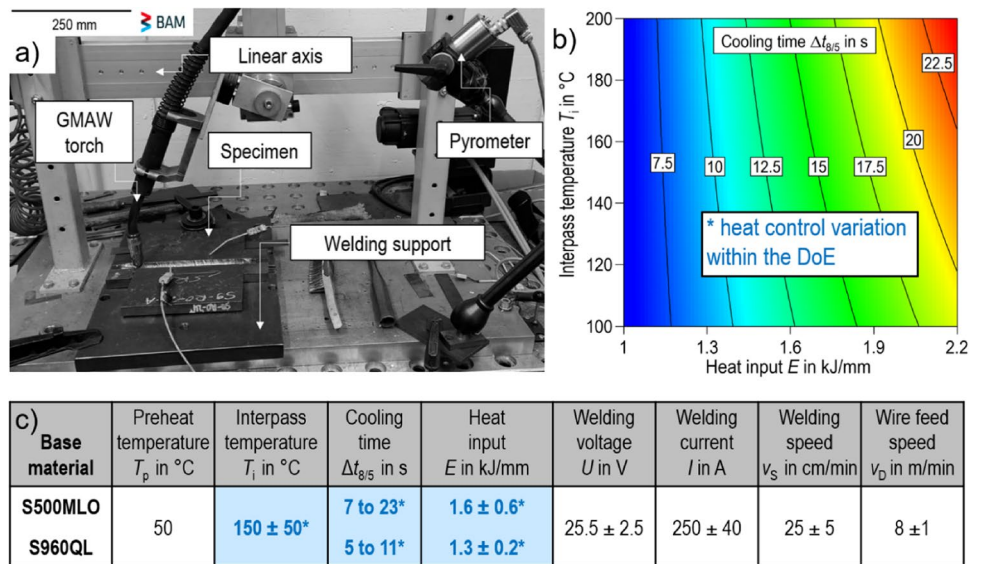


Fig. 5 Parameter matrix (design of experiments—DoE) for the repair welding tests

gouging at the seam flank in the base metal (or original weld HAZ) as well as in the non-gouging weld metal. In contrast to the affected areas of the gouging groove of the S960QL, cf. Figure 7g, the thickness of the HAZ of the S500MLO is significantly smaller with about 1 mm at the gouging flanks and about 0.5 mm at the gouging ground. This is due to the lack of preheating and somewhat lower power during gouging, cf. Section 2.2. Figure 7c shows the superposition of the original weld HAZ in the base metal with the affected area due to gouging. It is noticeable that here, a significantly lower hardness is caused near the joint flank compared to the areas in the weld metal influenced by the gouging. The individual HAZ areas (CGHAZ, FGHAZ, ICHAZ, tempering zone (SCHAZ)) are less pronounced and show a lower expansion. It is worth

mentioning that the base material S500MLO contains only 0.05% carbon in contrast to S960QL with 0.16%. Therefore, it can be assumed that in S500MLO, the increase in hardness is lower in comparison to the higher strength steel S960QL. A significant increase in hardness or gradients would have a detrimental effect on the possible recurrence of defects during repair welding. In addition, no defects, such as micro-cracks, are visible on the joint flank surface. A possible enrichment of the surface with carbon should be considered by appropriate mechanical finishing steps, such as grinding or pressure air hammering, to remove any layers with an increased carbon content or layers influenced by carbon.

Furthermore, the gouging of the HAZ in S960QL/G89 shows an approximately 1 mm wide significantly hardened

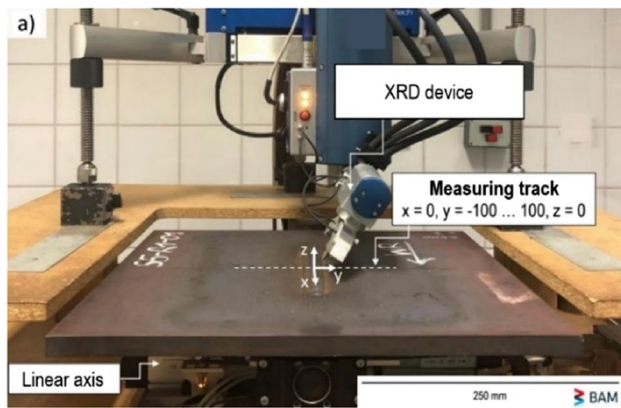


Fig. 6 XRD setup for residual stress analysis (transverse to the weld) of repair welded specimens

(up to more than 450 HV0.5) area, cf. Figure 7h. Between the hardened area and the unaffected base material, an up to 1 mm wide hem with a slightly lower hardness compared to the base material is visible. Analogous to Fig. 7c, Fig. 7g shows the metallographic examinations on the basis of a transverse section (etching with 2% Nital) with the respective HAZ due to gouging at the seam flank in the base metal and in the non-gouged weld metal. It can be seen that coarse-grained areas of the HAZ of the original weld are included in the HAZ of the thermal gouging. These areas, particularly characterised by high hardness, may have an especially negative effect during repair welding regarding the risk of cracking and subsequent component performance, especially in the case of such high-strength steel grades like S960QL. The risk of creating a greater number and severity of such critical areas is significantly increased by multiple repairs. The HAZ has a recognisable thickness of up to 1.5 mm at the joint flank and about 1 mm at the groove base.

3.2 Stress relieve due to gouging

A distinct reduction in residual stress after gouging can be observed, especially for the specimens with impeded transverse shrinkage, cf. Figure 8.

It should be noted, however, that gouging to a depth of approx. 50–70% of the seam height does not lead to a complete relaxation of the observed reaction forces due to the remaining root layer, even with a high restraint intensity. The reduction of the reaction stresses caused by gouging seems to be higher on the S500MLO/G50 than on the S960QL/G89 slot specimens based on the residual stress measurements on the top of the specimen despite the shorter gouging length. On the one hand, the reaction stresses were higher for the S500MLO compared to the S960QL, especially in the area of the HAZ. This could be observed reproducibly in several measurements after gouging in preparation for the repair welding test specimens.

3.3 Repair welding results

Figure 9a shows the weld structure and hardness distribution of the repair weld of the test material combination S500MLO/G50 when using the centre point parameters with an average cooling time of $\Delta t_{8/5} \approx 13$ s together with the hardness distributions for the lowest and highest heat input as well as interlayer temperature (or lowest and highest $\Delta t_{8/5}$ cooling times, respectively) of the parameter matrix. Likewise, these results are shown in Fig. 9b for the repair welds of S960QL/G89.

Overall, the repair welds show a significant increase in the width of the weld and HAZ compared to the original weld, cf. [1], and, especially in the case of S960QL/G89, a hardening in the HAZ of the cap layer and the HAZ within the weld metal with values of up to 450 HV0.5 and over 380 HV10, respectively. Particularly critical due to high hardness and notch effect is the area of the undercut, which, as shown in the experiments, can overlap with hardened areas influenced by gouging and the intercritical heated zones by the cap layer welding. When introducing the weld metal during repair welding, such areas must therefore be sufficiently well detected and avoided by appropriate tempering. The S500MLO does not show any areas with such a significant increase in hardness. Both test materials show a wide HAZ with low hardness in the area of the root, which has to be examined with regard to not meeting the required strength of the welded joints. Inclusions especially at the fusion line of the repair weld are to be avoided by careful reworking of the joint flanks. The width and shape of the HAZ clearly depends on the heat control. At low cooling rates, a wide HAZ with an extended area of low hardness is present. The cooling rates in the upper range of the parameter range lead to a clearly increased hardness in the weld metal and the HAZ of the filler and cap layers, which results in particularly high hardness values of over 460 HV0.5 in the case of the high-strength S960QL/G89. It should be noted that $Dt_{8/5}$ cooling times of 5 s and below can cause hard crack-critical microstructures or considerably reduced strain reserves of the weld and may reduce the crack safety in the course of repair welding. Ultimately, defect-free repair welds could be achieved with all the heat control parameters investigated. In the case of S960QL/G89, however, $\Delta t_{8/5}$ cooling times of more than 10 s can lead to the required strength or tensile strength (min. 980 MPa according to the base material) not being achieved in the welded joint.

3.4 Repair welding residual stresses

Figures 10a and b show transverse residual stress profiles after welding, gouging and repair welding for the medium and high restraint condition of self-restrained specimen types P2 and P3, respectively, for S500MLO/G50. It is evident that the higher restraint in the transverse direction of

Fig. 7 Gouging groove (**a, e**), cross-sections (**b, f**), detail of gouging HAZ (**c, g**), hardness maps (**d, h**) of gouged, non-mechanically post-treated, free-shrinking welds of S500MLO/G50 (**a-d**) and S960QL/G89 (**e-h**)

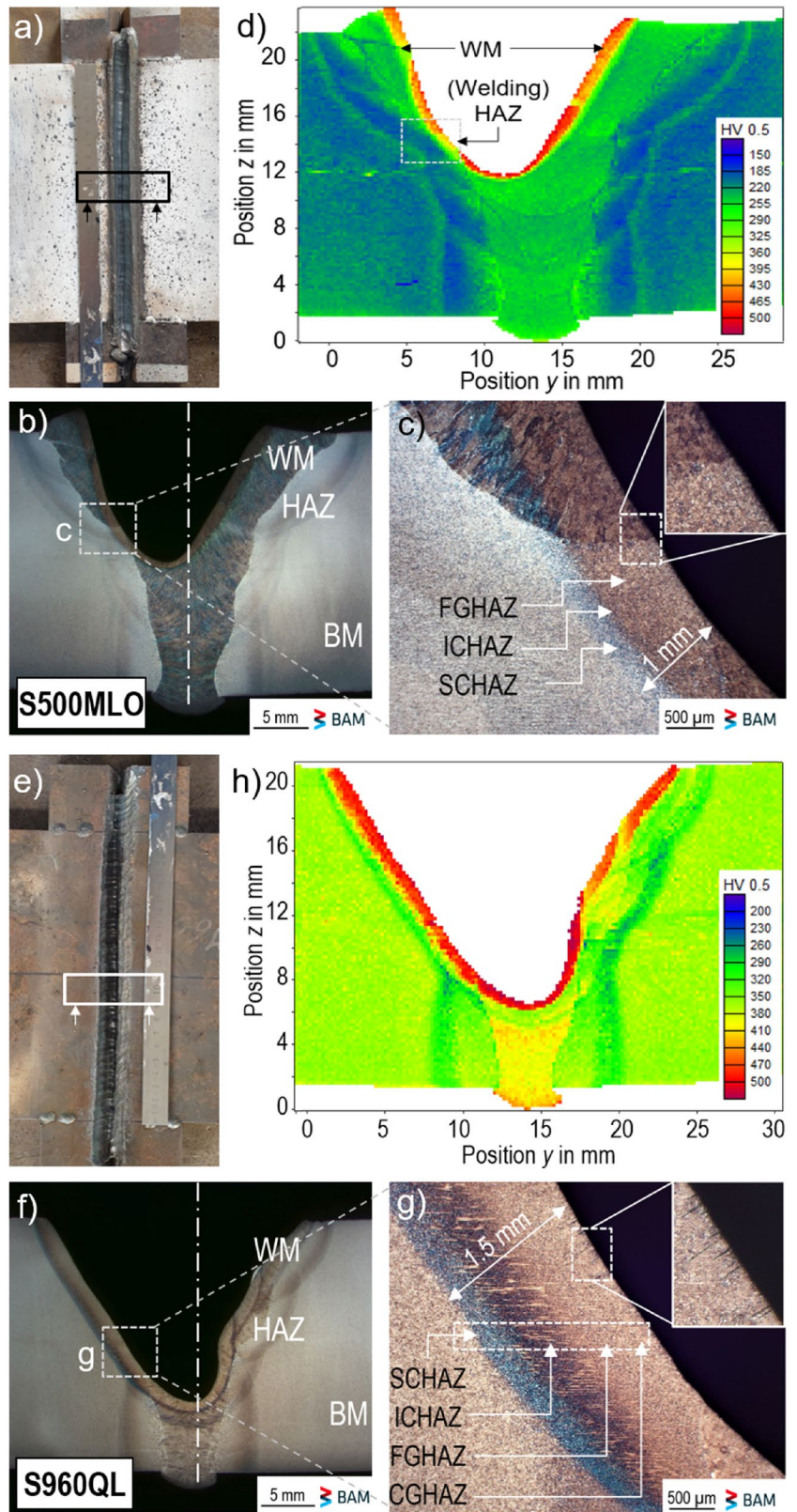
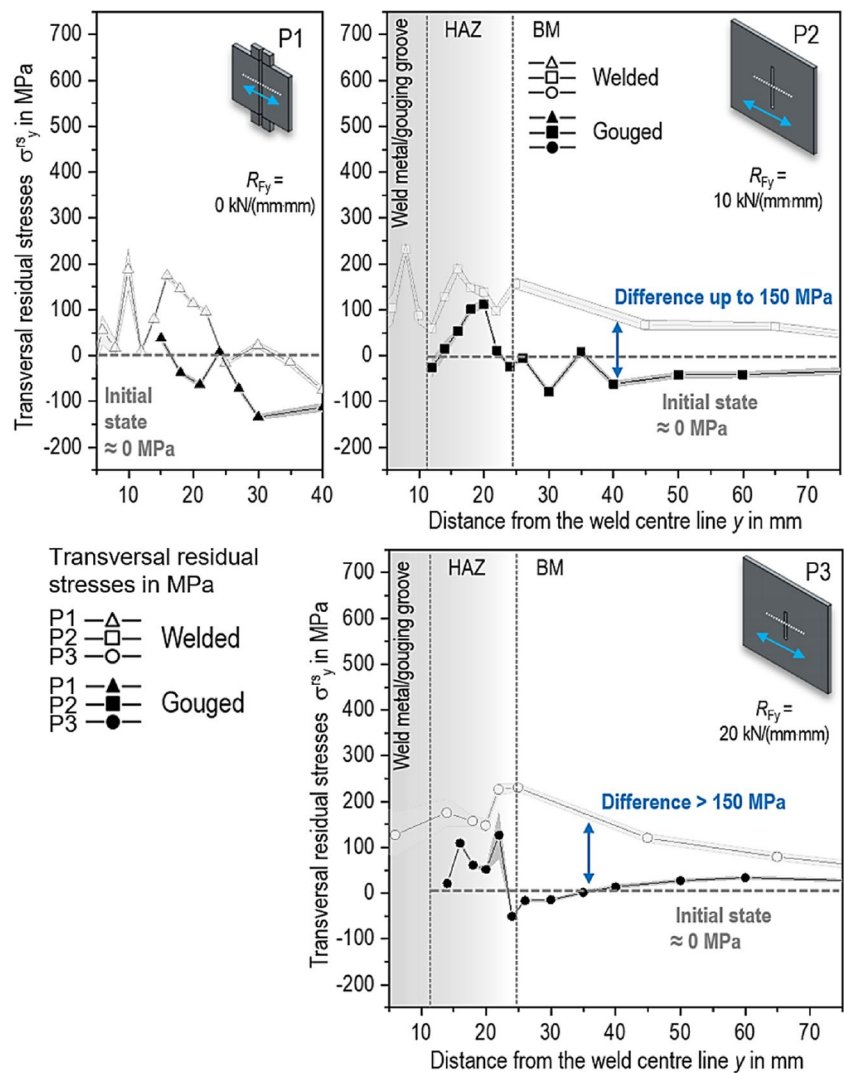


Fig. 8 Transverse residual stresses $\sigma_y^{rs}(y)$ before and after gouging (specimens P1–3, S500MLO/G50)



the weld causes higher transverse residual stresses in the welded and repair-welded specimens, especially in the HAZ and the base material. The gouging also causes a significant reduction of the transverse residual stresses in these areas to a similar level in the specimens P2 and P3, although the initial state is not reached due to the remaining root weld after gouging. The repair welding initiates a significant increase of the welding-induced stresses. Due to the higher restraint intensity in specimen P3 compared to P2, the corresponding support effects in HAZ and base material lead to significantly increased residual stresses. Likewise, Fig. 10c presents the transverse residual stress profiles after welding, gouging and repair welding for the high restraint specimen P3 of the steel grade S960QL/G89. Here, too, it is obvious that the high restraint condition in the transverse direction of the weld leads to increased transverse residual stresses, especially in the HAZ and in the base material at the seam.

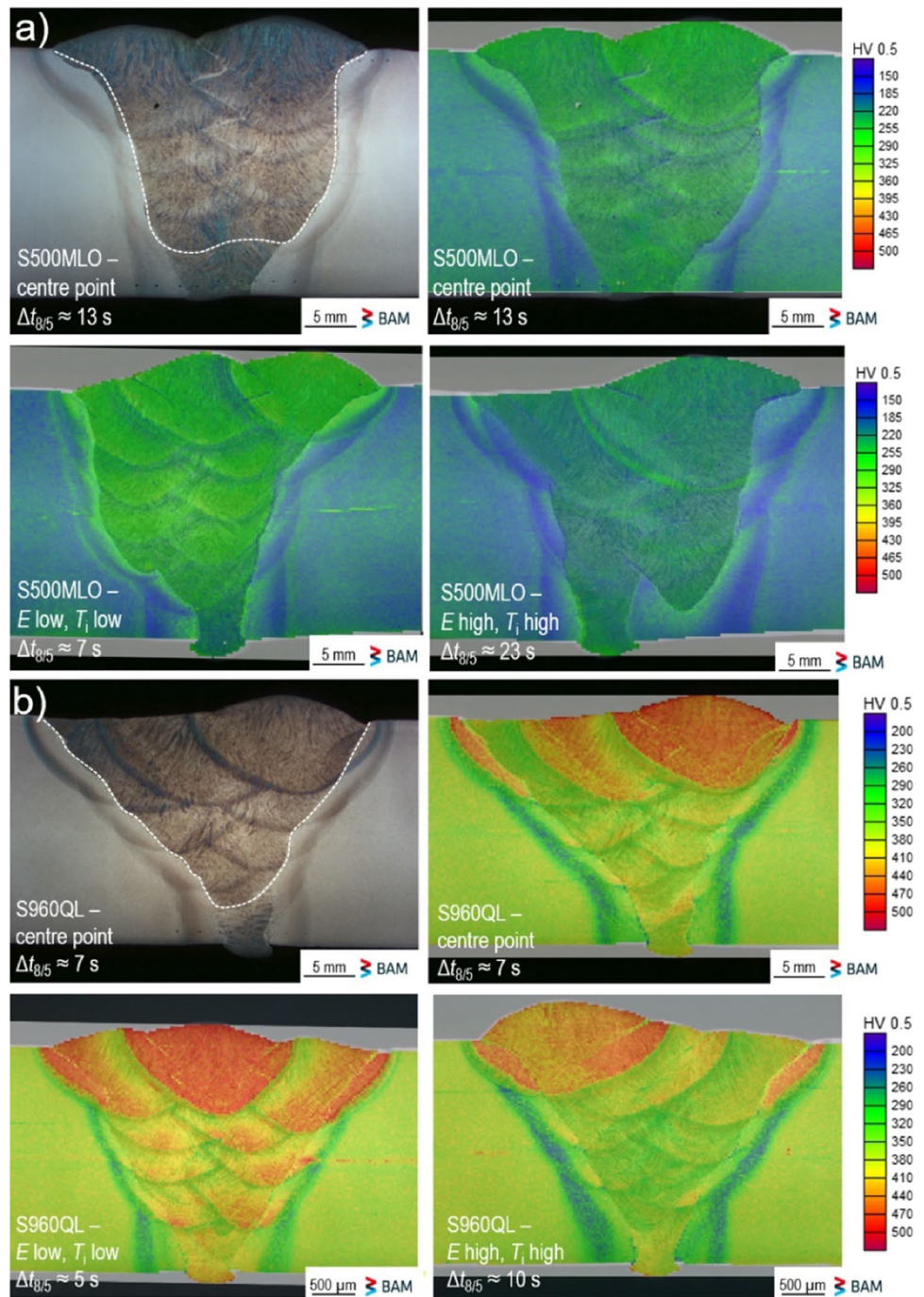
For the following presentation of the results with regard to the effects of heat control and restraint intensity or steel

grade, residual stress levels or average residual stresses are given for individual areas (weld metal, HAZ, base material). These can be calculated using the formula shown in Fig. 10d based on the individual values of the line measurement over the weld seam and weld vicinity.

The influence of heat control is exemplified in Fig. 11 based on transverse residual stress profiles for repair welds on S960QL/G89-P3 slot specimens for two different interpass temperatures and heat input values.

At constant heat input, cf. Figure 11a, the increase of the interpass temperature shows a significantly higher residual stress level in the HAZ and in the base metal due to reaction stresses resulting from the high restraint conditions. According to well established concepts [21–24], welding at a higher temperature level after finishing the cap layer leads to a significantly higher quantity of heat in the weld region, which causes a higher shrinkage in connection with an initiation of significantly higher shrinkage forces due to the restraints when the weld is cooled down to room

Fig. 9 Cross sections and hardness maps for repair welds with centre different heat controls (minimum, medium and maximum) cooling times or heat control parameters. S500ML/G50 (a). S960QL/G89 (b)



temperature. The observed influence of the heat input, in contrast, is less pronounced, cf. Figure 11b. Thus, at higher heat input values and constant interpass temperature, the maximum residual stresses and stress gradients in the weld metal are partly lowered. Furthermore, a decrease in the residual stress maxima in the HAZ is evident at higher heat input values, which, according to other studies [10], results from the different layer build-up with a lower number of weld beads, which ultimately leads to reduced initiation of bending moments and stresses during welding and cooling.

The multitude of local effects that influence the development of residual stresses, especially in the case of multilayer welding of transformable steels in the area close to the surface, impedes the quantification and comparability of the welding residual stresses, especially in the case of repair welding. It can be assumed that, in principle, the reaction stresses are superimposed on the residual stress profile in the weld metal. Differences in the heat input, i.e., also in the weld bead volume, lead to a different build-up of the filler and cap beads and corresponding tempered areas or to a different

Fig. 10 Transverse residual stress profiles $\sigma_y^{rs}(y)$ after welding, gouging and repair welding on slot specimen P2 (medium restraint intensity, S500MLO/G50, **a**) and P3 (high restraint intensity, S500MLO/G50, **b**; S960QL/G89, **c**). **d** Calculation of residual stress level for certain weld areas according to [9]

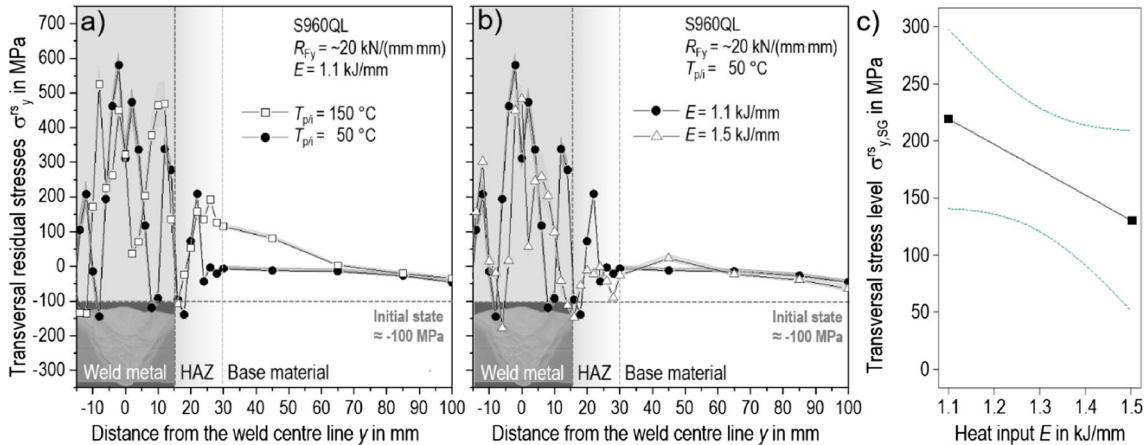
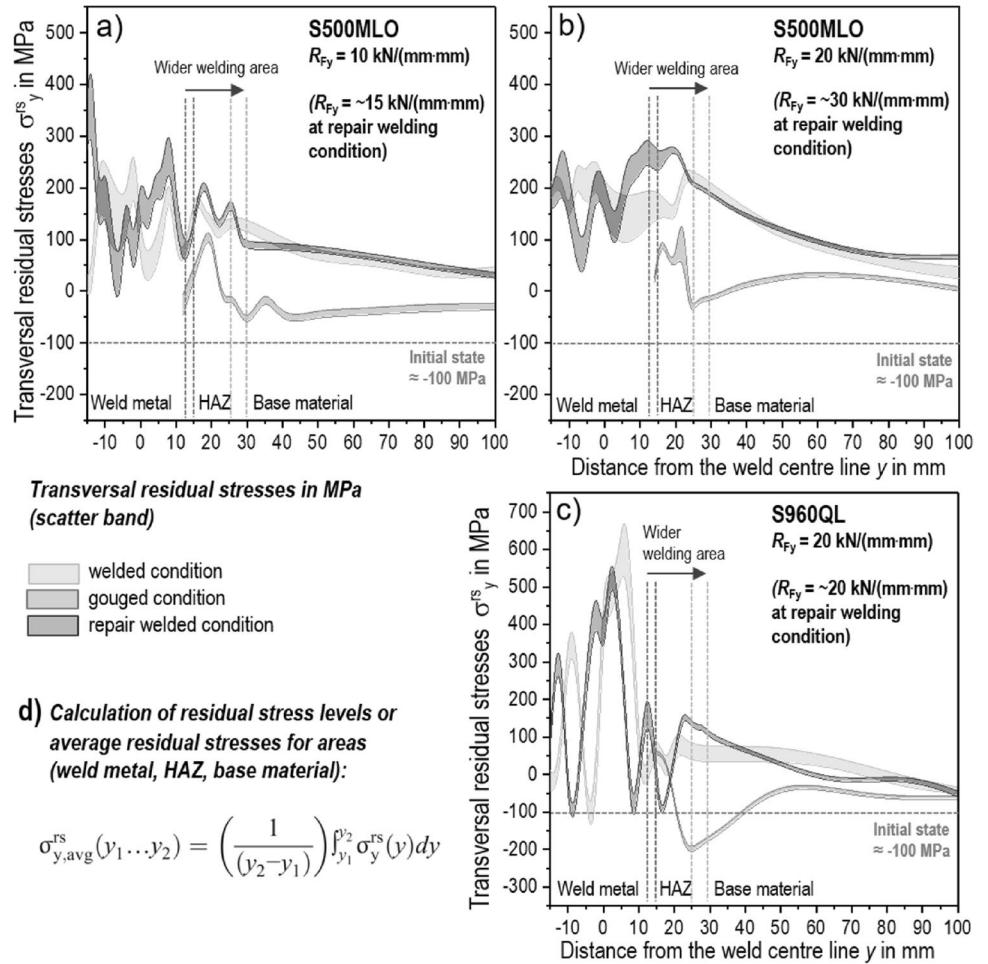


Fig. 11 Transverse residual stress profile $\sigma_y^{rs}(y)$ of repair-welded slot specimens P2 from S960QL for different interpass temperatures (**a**) and heat inputs (**b**). **c** Average transverse residual stresses of the weld

metal $\sigma_{y,SG}^{rs}$ vs. heat input E of all the repair welded specimens from S960QL/G89 (linear regression)

development of quenching effects and inhomogeneous transformation, which can result in high residual stress gradients, see [10, 24]. Due to the large number of measurements, the

residual stress level in the weld metal is comparatively scattered in the investigated parameter range, cf. Figure 11c. Nevertheless, with a model quality of approx. $R^2 = 47\%$, a

trend can be observed that higher heat input values cause a lower residual stress level in the weld metal for S960QL/G89 steel grades.

3.5 Effect analysis on residual stresses

With the help of a statistical evaluation of the analysed residual stresses, regression models could be developed for the different weld areas with regard to the effects of heat control and restraint intensity on the welding-related stresses. The influence of the heat control and restraint intensity on the residual stress level in the HAZ is shown in Fig. 12 by means of contour plots for S500MLO/G50 (a) and S960QL/G89 (b) repair welds.

At the standard significance level of 5%, for the S500MLO/G50 repair welds, the factors of interpass temperature and restraint intensity are highly significant, and the heat input is not significant due to higher scatter. The model quality of the regression model is $R^2 = 92.9\%$ and is lower compared to the tests with S960QL due to the non-significance of the heat input. Figure 12a shows the clear correlation and high intensity of the effect with increased

residual stresses at higher interpass temperatures. The lowest stresses occur at low interpass temperature and heat input. However, the trend of increasing residual stresses in the HAZ at higher heat input is not significant because, in addition to heat input and weld bead size, the associated individual layer build-up at the selected heat input values is relevant [10, 24], as shown in Fig. 11. This can be attributed to the different heat control parameter set for S500MLO/G50 and the different transformation behaviour of weld metal and base metal (compared to S960QL/G89) in connection with the complex interaction during residual stress formation.

With increasing structural shrinkage restraint, the welding-induced stress on the HAZ expectedly increases almost proportionally. Within the regression model of S960QL/G89, cf. Figure 12b, with a high model quality of $R^2 = 98.5\%$, the effects of heat input, interpass temperature, restraint intensity and the interaction of heat input and interpass temperature are significant. As already discussed above, with the transverse residual stress profiles, cf. Figure 11, it becomes apparent that increased interpass temperatures lead to higher residual stresses in the HAZ, and that this increase

Fig. 12 Contour plots of the average transverse residual stresses of the base material adjacent to the weld and HAZ $\sigma_{y,HAZ}^{rs}$ vs. heat input E or restraint intensity R_{Fy} and interpass temperature T_i of repair welded specimens made of S500MLO (a) and S960QL (b); statistical evaluation/regression, level of significance 5%: **a** S500MLO, $R^2 = 91.7\%$; significance, $p(E) = 0.8541$, $p(T_i) = 0.043$, $p(R_{Fy}) = 0.001$; **b** S960QL, $R^2 = 98.5\%$; significance, $p(E) = 0.031$, $p(T_i) = 0.008$, $p(R_{Fy}) < 0.001$, $p(E T_i) = 0.037$

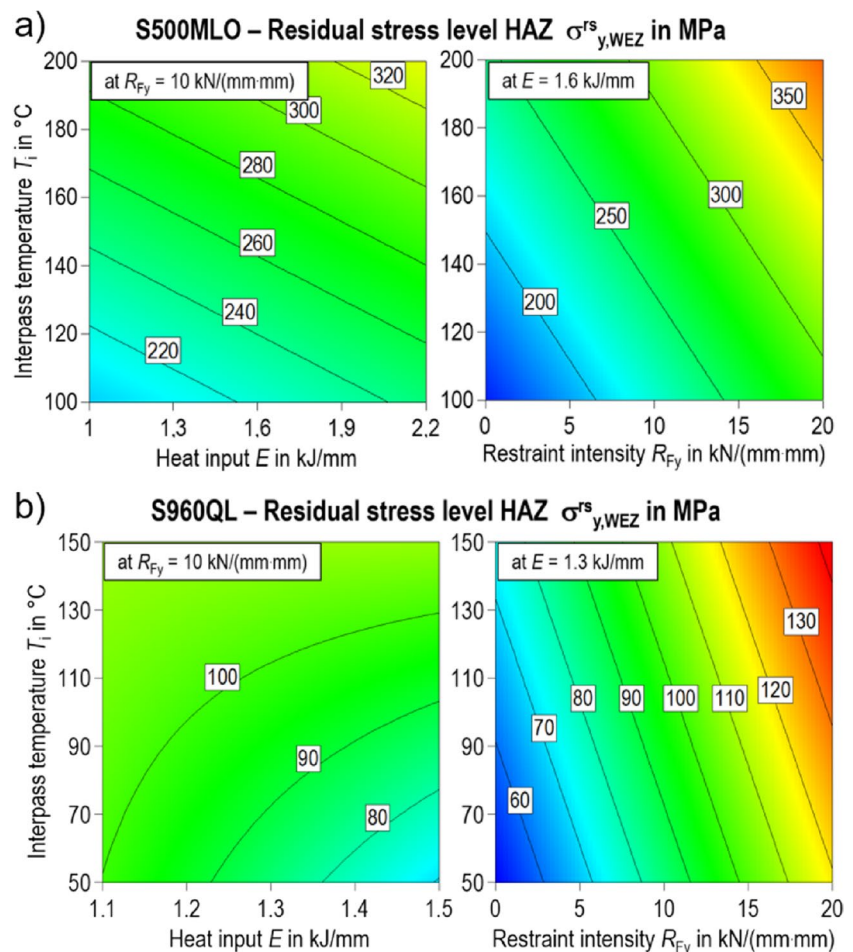
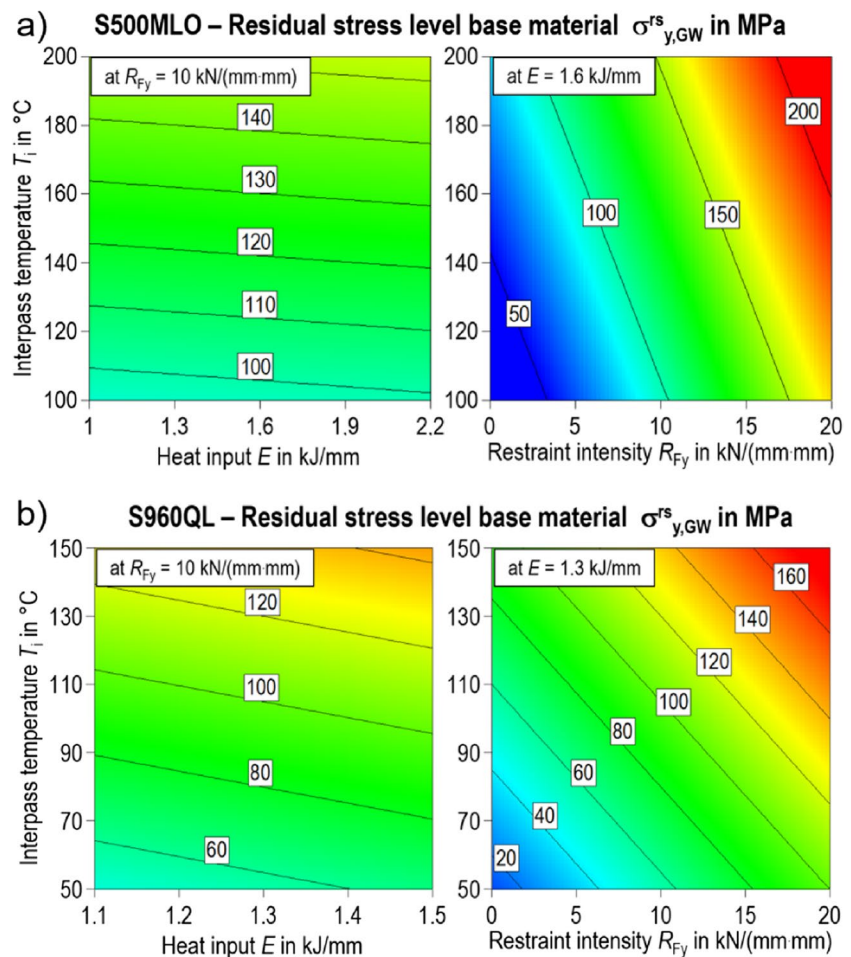


Fig. 13 Contour plots of the average transverse residual stresses of the base material adjacent to the weld and HAZ $\sigma_{y,GW}^{rs}$ vs. heat input E or restraint intensity R_{Fy} (b) and interpass temperature T_i of repair welded specimens made of S500MLO (a) and S960QL (b); statistical evaluation/regression, level of significance $p=5\%$: a S500MLO, $R^2=91.7\%$; significance, $p(E)=0.8541$, $p(T_i)=0.043$, $p(R_{Fy})=0.001$; b S960QL, $R^2=88.8\%$; significance, $p(E)=0.467$, $p(T_i)=0.009$, $p(R_{Fy})=0.006$



is greater the lower the heat input is. The lowest stresses occur at low interpass temperature and high heat input. This interaction was already observed in other component-related welding tests on the high-strength steel S960QL and is now also confirmed in repair welding [10]. With increasing structural shrinkage restraint, the weld-related stress on the HAZ increases almost proportionally.

The transverse residual stress level in the base material behaves similar for the two test materials S500MLO/G50, cf. Figure 13a and S960QL/G89, cf. Figure 13b. For the heat input, a comparatively low effect intensity in the selected parameter matrix and no significance can be observed. The residual stresses in the base metal near the welding area are primarily determined by the superposition of the reaction stresses due to the supporting effects of the restraint, which, as already discussed, depend essentially on the interpass temperature, and the restraint intensity. Both factors show significance within the regression model. The restraint intensity is indeed highly significant for both steel grades.

The model quality with $R^2=91.7\%$ for S500MLO/G50 test is comparable to the tests on S960QL/G89 ($R^2=88.8\%$) due to the non-significant effects of the heat input for both

steel grades. The contour plots show that a reduction of the interpass temperature in the entire parameter space causes a decrease of the resulting surface reaction stress. Lowering the interpass temperature from 200 to 100 °C for the S500MLO resulted in a 50 MPa reduction. For the S960QL/G89 material, lowering the temperature from 150 to 50 °C resulted in a decrease of the stress level by approx 70. MPa up to 80 MPa.

4 Conclusions

In order to develop stress-appropriate and safe repair concepts for high-strength steel welds based on scientific findings, gouging and repair welding tests were carried out by means of numerical, experimental component and stress analyses in part 1 of this research [1]. The following conclusions can be drawn from the results of the study in part 2:

1. The thermal gouging by means of carbon arc gouging especially in case of high shrinkage restraint and the resulting increased welding-induced stresses leads to a significant reduction of those residual stresses. When

- gouging to a depth of approx. 50–70% of the weld height, no complete relaxation of the reaction forces and stresses can be observed due to the remaining weld cross-section or root weld. Compared to the higher strength S960QL/G89, the grade S500MLO/G50 shows a greater reduction of the stress level on the upper side of the specimen for the test boundary conditions selected in the study. This is due to higher reaction stresses in the S500MLO/G50 (original weld) and the lower strength of the weld metal at elevated temperatures.
2. Carbon arc gouging, especially in the case of the higher-strength S960QL, causes pronounced affected areas on the joint flank with a distinct higher hardness and higher hardness gradients, which may be evidence of adverse effects on the microstructure and properties as well as possible surface defects on the joint flanks. This must be taken into account by means of mechanical reworking of the gouge grooves as well as by taking utmost caution in the welding repair.
 3. Compared to the original weld, the repair welds reveal significantly wider welds and HAZs and, in the case of the S960QL/G89, harder areas in the HAZ of the cap bead and in the weld metal. Width and characteristic of the HAZ depends on the welding heat control. Higher cooling rates effect narrower HAZs. Critical due to high hardness and notch effect is the area of the undercut, which may overlap with hardened areas due to gouging and the intercritical heated zones caused by the cap bead welding. During repair welding, such areas should be adequately addressed by tempering. In the area of the root, a wide HAZ with low hardness may occur, which should be inspected regarding compliance with the required weld joint strength. Defects, such as inclusions at the fusion line of the repair weld, are to be avoided by careful reworking of the root flanks.
 4. The cooling rates in the upper range of the investigated parameter window led to a significantly increased hardness in the weld metal and the HAZ of the filler and cap layers. This causes very high hardness values of > 460 HV0.5, especially for the high-strength steel grades S960QL/G89 and may cause crack critical microstructures or significantly reduced strain reserves. The heat control parameters examined in the study consistently resulted in defect-free repair welds. In the case of high-strength steel grades, however, exceeding the recommended cooling times is just as critical with regard to falling below the required strength of the welded joint.
 5. The welding stresses of the repair welds are increased compared to the original weld, especially in the areas of the HAZ and the base metal close to the weld. This is primarily due to the increased restraint conditions caused by the remaining root weld and/or shorter gouge grooves. In agreement with earlier investigations, the residual stresses across the weld seam can be significantly reduced by using upwardly limited working or interpass temperatures, as these reduce the reaction stresses, especially at high restraint intensities [25, 26].
 6. Furthermore, for the high-strength steel S960QL/G89, it is shown that with increasing welding heat input energy (rate of deposition), a significant reduction of the residual stresses in the HAZ can be achieved due to the reduction of weld beads, especially off-centre weld filler beads, at a low interpass temperature. Likewise, the data averages of all welding experiments show a trend that residual stress gradients and maxima in the weld metal may be reduced with higher heat input. However, the influence of the heat input is small compared to the interpass temperature for both test materials and is primarily suitable for adapting the layer build-up and cooling time in accordance with previous studies.
 7. Finally, it is recommended that the depth and length of the gouging as well as the gouging method (thermal or mechanical) is adequately selected depending on the defect situation, in order to achieve longest possible, flat and narrow grooves on the one hand and, thus, the highest possible reduction of the welding-related stresses on the other, as it was already stated in the study of [18]. This is all the more important the higher the constructive rigidity of the surrounding structure is, in such cases if the repair concept does not allow for constructive measures by prior disassembly.

Acknowledgements The IGF project No. 20162N (FOSTA P1311) of the Research Association for Steel Application (FOSTA) were supported by the Federal Ministry for Economic Affairs and Climate Action by the AiF as part of the programme for support of the cooperative industrial research (IGF) on the basis of a decision by the German Bundestag. We would like to thank for this funding, and the companies involved in the project committees for their support

Supported by:



on the basis of a decision
by the German Bundestag

Funding Open Access funding enabled and organized by Projekt DEAL.

Declarations

Conflict of interest The authors declare no competing interests.

Open Access This article is licensed under a Creative Commons Attribution 4.0 International License, which permits use, sharing, adaptation, distribution and reproduction in any medium or format, as long as you give appropriate credit to the original author(s) and the source, provide a link to the Creative Commons licence, and indicate if changes were made. The images or other third party material in this article are included in the article's Creative Commons licence, unless indicated otherwise in a credit line to the material. If material is not included in

the article's Creative Commons licence and your intended use is not permitted by statutory regulation or exceeds the permitted use, you will need to obtain permission directly from the copyright holder. To view a copy of this licence, visit <http://creativecommons.org/licenses/by/4.0/>.

References

- Schroepfer D, Witte J, Kromm A, Kannengiesser T (2024) Stresses in repair welding of high-strength steels—Part 1: Restraint and cold cracking risk. *Weld World* 68:685–697. <https://doi.org/10.1007/s40194-024-01691-y>
- Beiter P, Rand JT, Seel J, Lantz E, Gilman P, Wiser R (2022) Expert perspectives on the wind plant of the future. *Wind Energy* 25:1363–1378. <https://doi.org/10.1002/we.2735>
- Keehan E, Karlsson L, Andren HO, Bhadeshia HKDH (2006) New developments with C-Mn-Ni high-strength steel weld metals — part B. *Mech Properties Weld J* 09:218–224
- Schasse R, Kannengiesser T, Kromm A, Mente T (2015) Residual stresses in repair welds of high-strength low-alloy steels. *Weld World* 59:757–765. <https://doi.org/10.1007/s40194-015-0257-9>
- Guyot S, Dubois JM, Bryla P (2009) Welding reparation on thermo-mechanical HSS. In: Conference on high strength steels for hydropower plants. Japan Electric Power Civil Engineering Association, Takasaki
- Bae DH, Kim CH, Cho SY (2002) Numerical analysis of welding residual stress using heat source models for the multi-pass weldment. *KSME Int J* 16:1054–1064. <https://doi.org/10.1007/BF02984424>
- Jiang W, Xu XP, Gong JM, Tu ST (2012) Influence of repair length on residual stress in the repair weld of a clad plate. *Nucl Eng Des* 246:211–219. <https://doi.org/10.1016/j.nucengdes.2012.01.021>
- European Standard EN 1011-2 (2001) Welding - recommendation for welding of metallic materials - Part 2: Arc welding of ferritic steels
- Schroepfer D, Kromm A, Kannengiesser T (2017) Engineering approach to assess residual stresses in welded components. *Weld World* 61:91–106. <https://doi.org/10.1007/s40194-016-0394-9>
- Schroepfer D, Kromm A, Schaupp T, Kannengiesser T (2018) Welding stress control in high-strength steel components using adapted heat control concepts. *Weld World* 63:647–661. <https://doi.org/10.1007/s40194-018-00691-z>
- Sun J, Hensel J, Nitschke-Pagel T, Dilger K (2019) Influence of restraint conditions on welding residual stresses in H-type cracking test specimens. *Materials* 12:2700. <https://doi.org/10.3390/ma12172700>
- Schroepfer D, Kannengiesser T (2014) Correlating welding reaction stresses and weld process conditions for high-strength steel S960QL. *Weld World* 58:423–432. <https://doi.org/10.1007/s40194-014-0127-x>
- Keehan E, Karlsson L, Andren HO, Bhadeshia HKDH (2006) New developments with C-Mn-Ni in high strength steel weld metals — part A. *Microstructure Weld J* 09:200–210
- Wongpanya P, Boellinghaus T, Lothongkum G (2008) Ways to reduce the cold cracking risk in high strength structural steel welds. Safety and reliability of welded components in energy and processing industry - Proceedings of the IIW International Conference, Graz, Verlag der Technischen Universität
- Sun J, Nitschke-Pagel T, Dilger K (2023) Generation and distribution mechanism of welding-induced residual stresses. *J Mater Res Technol* 27:3936–3954. <https://doi.org/10.1016/j.jmrt.2023.10.252>
- Grong Ø (1997) Metallurgical modelling of welding (Materials Modelling Series). 2nd edn. Institute of Materials, Maney Publishing
- Karpenko M (2001) Influence of the cutting gases during thermal cutting (PhD thesis, OVGU Magdeburg, in German), Shaker, Aachen
- Dong P (2018) On repair weld residual stresses and significance to structural integrity. *Weld World* 62:351–362. <https://doi.org/10.1007/s40194-018-0554-1>
- Satoh K, Nakajima H, Toyosada M (1972) Restraint intensity of weld joints in the structural members consisting of plates and stiffeners, IIW-Doc X-660-72
- Withers PJ, Bhadeshia HKDH (2001) Overview - residual stress part 1 - measurement techniques. *Mater Sci Technol* 17:355–365. <https://doi.org/10.1179/026708301101509980>
- Wohlfahrt H (1987) Residual stresses as a consequence of welding. In: *Advances in surface treatments*, vol 4. International guidebook on residual stresses. Pergamon, pp 40–58
- Nitschke-Pagel T, Wohlfahrt H (1991) The generation of residual stresses due to joining processes. In: *Residual stresses. measurement, calculation, evaluation*. DGM Informationsgesellschaft mbH, Oberursel, pp 121–133
- Withers PJ, Bhadeshia HKDH (2001) Overview - residual stress part 2 - nature and origins. *Mater Sci Technol* 17:366–375. <https://doi.org/10.1179/026708301101510087>
- Masubuchi K (1980) Analysis of welded structures: residual stresses, distortion, and their consequences. Pergamon
- Schroepfer D, Kromm A, Kannengiesser T (2015) Improving welding stresses by filler metal and heat control selection in component-related butt joints of high-strength steel. *Weld World* 59:455–464. <https://doi.org/10.1007/s40194-014-0219-7>
- Kannengiesser T, Lausch T, Kromm A (2011) Effects of heat control on the stress build-up during high-strength steel welding under defined restraint conditions. *Weld World* 55:58–65. <https://doi.org/10.1007/BF03321308>

Publisher's Note Springer Nature remains neutral with regard to jurisdictional claims in published maps and institutional affiliations.